

# 1. Materials and Methods

## 1.1. Magnetic Sensor Device

### 1.1.1. Assembly of Sensor

The fabrication of a microfluidic device on various substrates and layouts consists of two parallelizable workflows. First, the giant magneto resistance (GMR)-sensor chip (Sensitec GmbH, Lahnau, Germany) is assembled into a custom designed PCB (Piu-Printex) by double sided adhesive tape and a square glass slide (25 mmx25 mm, Thermo Scientific) at the bottom. The device is electrically contacted via wedge wire bonding (HB10, TPT) with an aluminium wire ( $\varnothing$  25  $\mu$ m). The optimal parameters are listed in table 1. However, crucial for successful wire bonding is the optimal hole shape in the welding

Parameters	Bond 1	Bond 2
Ultrasonic Power	250	300
Time / ms	200	200
Force / mN	250	300

**Table 1:** Wirebonding Parameters

tool. Therefore, it was cleaned when bonds failed for no obvious reason by removing the gold wire and dipping the tip of the wedge into isopropanol (IPA). Then, *Test USG* was alternated for several seconds in multiple iterations. Afterwards, the wedge was blown dry from all sides with pressurized air and the wire was loaded back into the tool. After wire bonding, the manufactured sensors were placed in a wafer shipper box and stored in a dust free environment for later use.

### 1.1.2. Design and Fabrication of Microfluidics

In the second workflow, a microfluidic channel was manufactured via photo- and soft-lithography and bonded to the magnetic sensors from 1.1.1.

#### Development of Layout

##### Patterning of Photoresist

3" (100) silicon wafers (Si-Mat) were dehumidified in a drying oven (UN30, Memmert) for 2 h at 150 °C to 180 °C. Then, immediately after they reached room temperature, they were placed centered inside a wafer spinner (WS-650-23B, Laurell Technologies). For the desired layer thicknesses 2 mL to 3 mL SU8-30XX (Microchem) were poured carefully onto the center of the wafer and the following program was carried out:

Foto of setup with arrows to necessary parts Microscope Stages PEEK holder Helmholtz coils Kepco MFLI DAQ Lock because of reduced velocity and magnetic drag Different produced GMR stacks Why stone Bridge setup Magnetic alignment

layout design, hier noch die mänder und verengungen den kapten 150u wafer?

1. 500 rpm for 10 s at  $100 \text{ rpm s}^{-1}$
2. 3000 rpm for 30 s at  $300 \text{ rpm s}^{-1}$
3. Ramp down at  $300 \text{ rpm s}^{-1}$

Upon finish, the wafer was gripped outermost with wafer tweezers and soft-baked on a hot plate (super nuova+, Thermo Scientific) for 5 min at  $65^\circ\text{C}$  and at least 10 min at  $90^\circ\text{C}$ . The optimal duration was determined if the gently touched resist did not stick to the tweezers. To prevent cracks in the resist caused by a fast temperature change, the wafer was cooled on the hotplate to room temperature. Such processed wafers were stored for a maximum of 4 weeks in a light-tight storage box.

To pattern the resist, the i-Line of a laser lithograph (Dilase 250, Kloe) was used. In preparation of the writing layout a AutoCADz \*.dxf-file with only one layer of polylines was imported to the program “Kloe Design”, converted to contours and subsequently to polygons. For the filling a spot-size equivalent to the minimal structure resolution (as measured in Hicsanmaz [1]) and an overlap of at least 50 % was chosen. Departure and End Stabilization were chosen to 0.5 mm in a horizontal infill pattern. Also, flags for *auto-reverse mode*, *apply multiple trigger*, and *detect partial/full overlap* have been set. The writing trajectories were displayed for a last control before the export to ensure only closed contours. Finally the contour and filling were exported into separate files.

Both files were loaded in this order into the program “Dilase 250”. Also the preprocessed wafer was placed inside the laser writer and attached to the vacuumed stage. With the integrated camera the global zero was set to the wafer center by finding the horizontal or vertical edges and adding/subtracting the radius of the wafer ( $1.5'' \approx \varnothing 38.1 \text{ mm}$ ). The focus point was set to the top of the resist and subsequently moved 0.07 mm relative down for thick layers. Then the program was initiated with 100 % laser modulation and  $20 \text{ mm s}^{-1}$  to  $40 \text{ mm s}^{-1}$  writing velocity.

### **Soft Lithography**

The fabricated wafer was placed the center of a 90 cm petri dish. A poly(dimethylsiloxane) (PDMS) mold was created by vigorous mixing of the pre-polymer base with its curing agent (Sylgard 184, Dowsil) in a ratio of 10:1 (w/w). For 3" wafers, thin channels were casted from 15 g, channels with standard thickness from 20 g PDMS in the petri dish. Gas bubbles were removed from the mixture in a desiccator for 20 min at 2 hPa, and the PDMS was cured in an oven (Um, Memmert) for 1 h at  $60^\circ\text{C}$ . After curing, the PDMS mold was released from the petri dish carefully, taken off the wafer and stored in a clean petri dish upon further processing.

### **Bonding of Microfluidics**

Under a laminar flow hood, crosslinked molds were cut into pieces with the respective single microfluidic ( $\mu\text{F}$ ) with a razor blade. Holes for in- and outlet were added with a biopsy puncher ( $\varnothing 0.5 \text{ mm}$ , WellTech). The substrates and  $\mu\text{Fs}$  were sonicated in

acetone and deionized water ( $\text{diH}_2\text{O}$ ) for 5 min, and dried with filtered nitrogen gas ( $\text{N}_2$ ) completely. For the bonding of PDMS to various substrates different protocols have been established:

### **PDMS Glueing**

Here, a micron-height layer of uncured PDMS was used as an adhesive layer between  $\mu\text{F}$  and substrate. Approx. 3 mL were poured onto a 3" wafer and spun down for 5 min at  $6000 \text{ min}^{-1}$ . The microchannel was placed on the substrate by visual control of a stereo microscope (SMZ800, Nikon) with 8-fold magnification. Subsequently, the bonding process could be finished by a 1 h bake at  $60^\circ\text{C}$  or over-night at room temperature.

### **Plasma Bonding**

The respective parts were activated by the exposure to a controlled oxygen gas ( $\text{O}_2$ )-plasma. Bringing the activated surfaces in contact immediately triggers the formation of covalent bonds. First, the acetone-wiped substrates and the microchannels were centered inside the plasma cleaner (Zepto, Diener). Second, vacuum was applied to a final pressure  $<0.2 \text{ hPa}$ . Third, the chamber was flushed with pure  $\text{O}_2$  until a chamber pressure from  $0.6 \text{ hPa}$  to  $0.8 \text{ hPa}$  had been stabilized. Fourth, the plasma process was executed with  $30 \text{ W}$  (Power-Potentiometer: 100) for 45 s to 60 s (Time-Potentiometer: 15-20). Upon finish, the chamber was flushed for 5 s and ventilated. Immediately after, the corresponding workpieces were brought into contact and pressed together gently. To ensure a durable bond, the assembled structures were baked for 1 h at  $60^\circ\text{C}$ .

### **Reversible Bonding**

To bond the  $\mu\text{F}$  to a substrate reversibly and without residues, the channel can be brought into contact with the bottom part without any adhesinon agent. For low-pressure as well as vacuum driven flows, this method is preferable due to its time and work efficiency.

#### **1.1.3. Peripheral Components and Optical Readout**

Each sensor chip was characterized by the hysteresis steepness (equivalent to the sensitivity) and the zero-crossing at half-maximum in a customized setup. Therefore, the underlying  $32 \times 27 \times 5 \text{ mm}$  NeFeB magnet (NE3227, IBS Magnet) was adjusted on micromanipulator tables (PT, Thorlabs) in three axes to optimize both parameters. Afterwards, PTFE-tubing (ID  $0.5 \text{ mm}$ , Reichelt Chemietechnik) was connected on the in- and outlet of the microfluidic. A dispensing tip (OD  $0.42 \text{ mm}$ , Nordson) was connected to the inlet tubing. Initially a  $1 \text{ mL}$  syringe (ID  $4.72 \text{ mm}$ , Terumo) was connected with  $\text{diH}_2\text{O}$  or phosphate buffered saline (PBS) and flushed with  $100 \mu\text{L min}^{-1}$  to  $200 \mu\text{L min}^{-1}$  by a syringe pump (Fusion 4000, Chemyx).

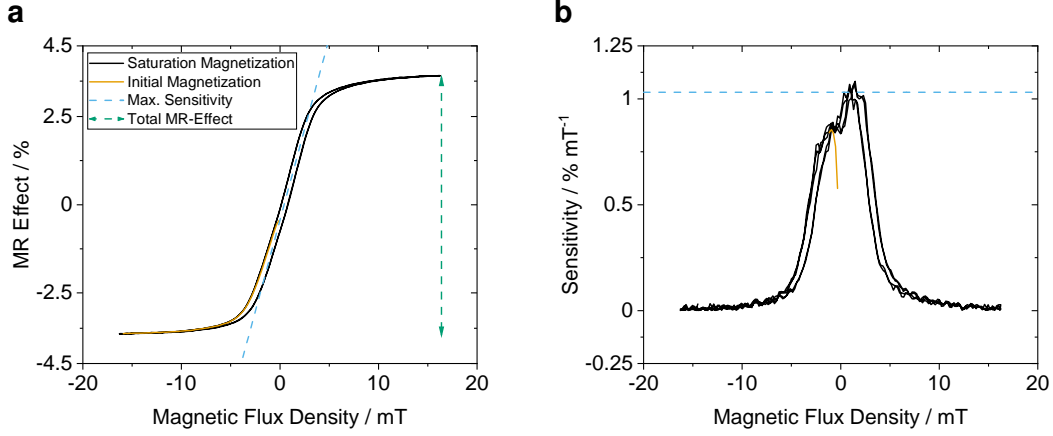


**Figure 1: Hysteresis Calibration of the GMR-Sensor**

Sensitivity Optimization of the GMR sensor via alternating hysteresis measurements and permanent magnet adjustment. (a) Optimal sensitivity is reached when the zero-crossing is centered around the zero-field and the linear section has the maximum steepness. (—) Upon dislocating the free layer in one direction, the magnetic field strength increases linearly towards saturation. (—) Afterwards, the magnetization moves on the hysteresis loop. The total magneto-resistive effect (MR effect) is calculated from the vertical distance between the saturation points. (—) (—) (b) In order to determine the steepness in the linear section, the hysteresis from the left side is differentiated. Actual sensitivity (—) is measured by the mean of all curves in the zero field. The initial magnetization curve is omitted from this measurement. (—)

### Hysteresis Alignment

For any used GMR-sensor, a characterization by its hysteresis was performed. (Fig. 1) Therefore, its hysteresis was imposed by two Helmholtz coils ( $L_s = 167 \text{ mH}$ ,  $d = 150 \text{ mm}$ , Brockhaus) generating  $7.8 \text{ mT A}^{-1}$  orthogonal to the easy axis of the GMR which were driven by a voltage-controlled current source (BOP 50-8M, Kepco Inc.) with  $\pm 2 \text{ A}$  at a peak-to-peak voltage ( $V_{pp}$ ) of  $20 \text{ V}$ . The control voltage was supplied by LabView (2018, 32-bit, National Instruments) supplied by a digital I/O card (USB-6351, National Instruments) in the range of  $-10 \text{ V}$  to  $10 \text{ V}$ . The resulting sensor signal was fed into the current input of a lock-in amplifier (multi frequency lock-in (MFLI),  $5 \text{ MHz}$ , Zurich Instruments). Re-digitization and processing was carried out by the same digital I/O card and LabView program as for the input control.

In effect, the sensitivity was computed from the hysteresis' steepness in the magnetic zero-field. Hereby, the very first hysteresis loop was omitted for further calculations because it contains the initial magnetization curve. (Fig. 1a) By differentiating the hysteresis (Fig. 1b), the maximum MR effect per unit magnetic field could be computed from the numeric maximum in  $x = 0$ . During the course of the thesis, it resulted typically in  $1.2 \pm 0.2 \% \text{ mT}^{-1}$ . From this, the bridge sensitivity could be also expressed in unit of  $\Omega \text{ mT}^{-1}$ . With a typical GMR resistance of  $300 \pm 50 \Omega$  and a supply of  $V_{pp} = 200 \text{ mV}$ , the typical voltage drop results in  $840 \pm 130 \mu\text{V mT}^{-1}$ .<sup>1</sup>

### Single GMR

The change in resistivity over one whole Wheatstone bridge was measured with a fully-integrated lock-in amplifier (MFLI,  $5 \text{ MHz}$ , Zurich Instruments) by a supply peak volt-

<sup>1</sup> Output Voltage of one bridge branch:  $V_{out} = \frac{R_{sig}}{R_{const} + R_{sig}} \cdot \frac{V_{pp}}{2\sqrt{2}}$

age ( $V_p$ ) of 100 mV to 800 mV. The reference frequency was chosen randomly in a range of  $100 \pm 25$  kHz such that any harmonics were avoided. The measured differential bridge balance was then demodulated and filtered with a time constant of 299.7  $\mu$ s by a third order low-pass filter and amplified by the factor 10 000. Subsequently, the processed signal was sampled at  $53.2 \text{ kS s}^{-1}$  from the MFLI and subsequently from an 16-bit analog-to-digital converter (USB-6351, National Instruments) with input range of  $\pm 10 \text{ V}$  and  $10 \text{ kS s}^{-1}$ .

During sensor operation, a 20x microscope image (DM2500M, Leica Microsystems) was captured by a CCD-camera (Grasshopper3, FLIR) and displayed in real-time to control the experiment.

### Dual GMR

For the measurement of two GMR-sensors simultaneously, the setup from 1.1.3 was duplicated in two different manners. However, the exact same settings in the device control software were crucial for successful measurements. In a first approach, the supply cable of one MFLI was split and fed into both sensors, while the bridge balance was evaluated by the same and an additional lock-in, both with the exact same settings. Consequently, the ground pin of the one sensor was the reference also for the other sensor and one ground pin was therefore left floating. This method posed the least cable length and therefore noise, but was also prone to cross-talking between the used BNC-cables respectively -connectors.

Second, two MFLI's were driven in a master-slave clock synchronization by the Multi-Device Sync function. Therefore, the *trigger out* and *clock out* ports on the backside of the master were connected to the slave's *trigger in* and *clock in* ports. Additionally, the *trigger out* was split by a T-connector piece in order to feed it also back into the master's *trigger in* port.

In both cases, the output of both lock-ins was directed to their respective *AUX 1* ports and connected to another LabView program by the previously mentioned DAQ-card.

### Differential Sensor Setup

In some experiments, two PCBs were stacked with nylon spacers (D01482, DURA-TOOL Corp, Taiwan) with various lengths 3 mm, 5 mm and 8 mm between their edges above the permanent magnet. Before the stacking, outlet tubing of the upper chip was connected to the inlet of the lower chip with the least dead volume possible. Then, immediately before assembly, the channels were flushed with buffer and were inspected to confirm the absence of gas-bubbles. After the final assembly, the hysteresis was adjusted for both sensors on various bridges consecutively. Measurements were performed as described in 1.1.3 with two completely independent lock-in amplifiers.

## GMR Data Analysis

Subsequent data analysis of the acquired streams from both two and one sensor measurements were modified by a custom labview VI to cut the first sample of the stream which was mandatory for the next step. Next, the characteristic signal patterns were detected in the continuous stream by the *GMR\_Tool\_227* by a rolling-mean thresholding method. The resulting \*\_ana.csv files were then processed by a custom Matlab script, which in turn computed averages and simple parameters of a single detected signal or whole measured, p.e. the total volume or the signal count therein. The Matlab script saved any analyzed data also in the \*.csv format which was finally plotted in Origin (2020b, OriginLab)

## 1.2. Magnetic Beadometry

Magnetic beads were measured in various manners. First, beads were pumped over substrates under microscope control (DM6, Leica Microsystems GmbH, Germany) with simultaneous image acquisition for count (LAS X, Leica Microsystems GmbH, Germany) and trajectory analyses (ImageJ Fiji, [2]). Second, beads were measured in buffer or diluted whole blood samples to determine their concentration in the magnetic flow cytometer. The previous measurements were then adapted to functionalized surfaces in order to detect a difference in concentration. In all experiments, teflon tubing (ID 0.5 mm, RCT Reichelt Chemietechnik GmbH + Co., Germany), dispensing tips (OD 0.42 mm, Nordson Deutschland GmbH, Germany), 1 mL syringes (ID 4.78 mm, Terumo Deutschland GmbH, Germany), a syringe pump (Fusion 4000, Chemyx Inc., USA) and a microfluidic channel with dimension 700  $\mu\text{m}$  x 150  $\mu\text{m}$  (width x height) were used.

### 1.2.1. Optical Particle Tracking

tif stack, user roi polygon cropped threshold, yen dark stack invert duplicated slice with beads on it subtracted it from stack trackmate LoG detector, blob vornothing 8 micron thres: 2.0 use median filter, subpixel localizaiton, hperstack, set color by snr, linear motion LAP tracker, initial motion radius 60um, search radius 30um, max frame 250

### 1.2.2. Absolute Concentration Measurement

Before every measurement, the initial bead concentration was determined meticulously in a Neubauer Improved counting chamber or by flow cytometry and adjusted between  $1\ \mu\text{L}^{-1}$  to  $10\ \mu\text{L}^{-1}$  in PBS with Tween 20 (PBST). Then, after the sensor was calibrated accordingly in the single or dual GMR-setup (Sec. 1.1.3), beads were pumped at a fixed flow rate of  $80\ \mu\text{L min}^{-1}$  and  $30\ \mu\text{L min}^{-1}$  through a channel with 150  $\mu\text{m}$  or 50  $\mu\text{m}$  height, accordingly. Either the previously mentioned plastic syringe or a 1 mL glass syringe (1001 TLL, Hamilton Bonaduz AG, Switzerland) was utilized in a syringe system for these experiments. The duration to attain statistical significance was specified by a minimal volume 300  $\mu\text{L}$  or a detection of at least 300 particles. Between samples,

the whole system was flushed with PBST at flow rates greater than  $150\ \mu\text{L min}^{-1}$  or  $60\ \mu\text{L min}^{-1}$ , respectively to  $150\ \mu\text{m}/50\ \mu\text{m}$  channel heights. Afterwards, signal streams were analyzed according to the procedure in Sec. 1.1.3.

### 1.2.3. Whole Blood Bead Spiking

For measurements in whole blood samples, 6 mL blood were drawn from test subjects in 7.5 mL, 2,2',2'',2'''-(ethane-1,2-diyl dinitrilo)tetraacetic acid (EDTA)-containing vials (S-Monovette Hämatologie, Sarstedt AG & Co. KG, Germany). Beads with precise concentrations were prepared according to Sec. 1.2.2 in PBS. Then, several dilutions of whole blood were created from the particle solutions and mixed carefully with a 1 mL micro-pipette or by inversion. The samples were subsequently measured at a fixed flow rate of  $40\ \mu\text{L min}^{-1}$  in a  $150\ \mu\text{m}$  channel. In between samples, the channel has been flushed with MACS running buffer (MACS) buffer at high flow rates as in Sec. 1.2.2. The best measurements arose from S48 chips with broad, 200 nm-high nickel-iron structures.

### 1.2.4. Bead Capture Assay

As prerequisite for the bead capture assay, the different self-biotinylated particles (Sec. 1.3.4) were diluted as for the concentration measurement in Sec. 1.2.2. Further, a GMR sensor was fabricated, loaded unspecifically with  $1\ \text{mg mL}^{-1}$  neutravidin, hysteresis aligned and connected in the single GMR setup (see 1.1.3). As first step, the bead adhesion was determined by finding the minimal flow rate at which non-biotinylated beads were still rolling freely and at second, by finding the maximal flow rate at which biotinylated beads were still notably captured, both by microscope observation and sensor signal analysis. The average flow rate of these two was consequently held constant over all experiments. Subsequently, beads with different surface coverages of biotin were pumped alternatingly through the channel and over the sensor. The generated data was analyzed after the standard protocol in 1.1.3.

## 1.3. Surface Bio-Functionalization

### 1.3.1. Surface Activation

To functionalize any silicon containing surface with Si–OH groups which the utilized silane could interact with, multiple surface activation pathways were explored. First, substrates were cleaned in hydrochloric acid (HCl):methanol (MeOH) and sulfuric acid ( $\text{H}_2\text{SO}_4$ ) before they were immersed in boiling water. Second, surface silanol groups were achieved by piranha immersion. Third a hydrofluoric acid (HF) dip and fourth a oxygen plasma treatment was tested.

For all methods, the following reagents were used:  $\text{diH}_2\text{O}$  ( $0.054\ \mu\text{S}$ , Merck MilliQ), acetone ( $>99.9\%$ , VWR International LLC, Germany), ethanol (EtOH) (absolute, VWR International LLC, Germany), MeOH ( $99.8\%$ , VWR International LLC, Germany), acetic acid (AcOH) (glacial, VWR International LLC, Germany), HCl ( $37\%$ , Merck KGaA, Ger-

many),  $\text{H}_2\text{SO}_4$  (95 % to 98 %, Merck KGaA, Germany), hydrogen peroxide ( $\text{H}_2\text{O}_2$ ) (30 % (w/w), Merck KGaA, Germany), HF (10 %, VWR International LLC, Germany)

### **Work Safety Remarks**

Before the work with one of the acid solutions was carried out, several safety measures were implemented. As any reacting acid solution becomes very hot immediately due to the exothermic reaction, every container should be placed inside a cooled water or ice bath. Additionally, the beaker as well as concentrated acid flasks should be gripped firmly by a laboratory stand to avoid a tip over. As the reactivity of chemicals is highly temperature-dependent, the solutions were processed further when they had been cooled to  $\leq 80^\circ\text{C}$ . It should be also noted that - as in every chemical reaction, but especially ones with  $\text{H}_2\text{SO}_4$  and HF - the acid was always poured into the other reactant to avoid splashing and boiling.

### **Plasma Activation**

For the plasma activation, process parameters similar to the PDMS bonding technique in ?? were chosen. After initial cleaning via sonication in AcOH and diH<sub>2</sub>O for 5 min each, the substrates were dried in N<sub>2</sub>-gas and placed inside the plasma chamber. The chamber was evacuated to a final pressure  $<0.2\text{ hPa}$  and then flushed with pure O<sub>2</sub> until a chamber pressure between 0.6 hPa to 0.8 hPa had been stabilized. Fourth, the plasma process was executed with 100 W (Power-Potentiometer: 300) for 300 s (Time-Potentiometer: 190). Upon finish, the chamber was flushed for 5 s and ventilated.

### **Hydrochloric-Sulfuric Acid Activation**

In order to degrease any glass or silicon nitride ( $\text{Si}_3\text{N}_4$ ) surface, a protocol according to Dressick et al. [3] was used. There, the surfaces were first sonicated in acetone and diH<sub>2</sub>O for 5 min. Afterwards these were immersed in a 1:1 (v/v) solution of HCl:MeOH for  $>30\text{ min}$ , rinsed with diH<sub>2</sub>O copiously and soaked in  $\text{H}_2\text{SO}_4$  for  $>30\text{ min}$  as well. Then, the samples were rinsed again in deionized water. To form silanol groups on the activated surface, the surfaces were finally immersed in  $>90^\circ\text{C}$  heated (SuperNuova+, Thermo Scientific) diH<sub>2</sub>O for at least 2 h.

### **Piranha Activation**

In this method, activation was carried out in a 1:7 (v/v) piranha solution at  $70^\circ\text{C}$  for 15 min to 30 min. After treatment, the samples were rinsed carefully with diH<sub>2</sub>O three times.

### **Hydrofluoric Acid Activation**

For HF activation of  $\text{Si}_3\text{N}_4$ , a protocol after Liu et al. [4] was reproduced. Acetone cleaned samples were immersed in 1 % aqueous HF for 2 min and rinsed with diH<sub>2</sub>O extensively afterwards without letting the surface dry at any time.



### 1.3.2. Chemical Surface Functionalization

Chemically activated surfaces were now coupled with 3-triethoxysilylpropan-1-amine (APTES) covalently. Therefore an aqueous silane solution was prepared from EtOH with volume fractions of 5 % diH<sub>2</sub>O, 0.5 % aqueous AcOH (pH 4.5) and 1 % APTES in this order. The samples were soaked immediately after their activation in the silane solution. The reaction was carried out for 2 h to 4 h at >40 °C or for 1 h at 70 °C. At finish, all specimens were rinsed with EtOH or sonicated for 5 min in absolute EtOH.

Then, the amine terminated surface modification was enhanced by a carbodiimide conjugation with poly(acrylic) acid (PAA) after Andree et al. [5]. As above, a reaction consisting of 1 mM 2-(N-morpholino)ethanesulfonic acid (MES) buffer (pH 6) with 1 mg mL<sup>-1</sup> PAA, 6 mM 3-(Ethyliminomethyleneamino)-N,N-dimethylpropan-1-amine (EDC) and 3 mM 1-Hydroxy-2,5-pyrrolidinedione (NHS) was activated for 15 min on a magnetic stirrer. Subsequently, the prepared samples were immersed in the solution for 1 h on a rotation shaker (VWR). As final cleaning, the slides were rinsed or sonicated for 5 min in diH<sub>2</sub>O and stored in fresh diH<sub>2</sub>O at 4 °C up to 14 d upon further use.

### Tensiometry

All above methods were characterized by a custom built tensiometer and the ImageJ Fiji plugin DropSnake. [2, 6] In an experiment, a substrate was dried by N<sub>2</sub> and placed in the camera focus. Subsequently, a sessile drop of 1 µL was placed in the focus with a micropipette (Eppendorf) without touching the surface. The focus of the camera was adjusted meticulously to gain maximum contrast at the droplet contour and a homogeneously black droplet. Images were then acquired by an USB-microscope pointing in an acute angle onto a drop on the surveyed substrate, while background illumination was provided by a lamp. The images were then cropped, rotated such that the droplet edges were perfectly horizontal and converted to 8-bit grayscale. After preprocessing, the top half contour was outlined by at least 8 points inside the DropSnake plugin and the resulting contact angles were exported.

usb microscope?

Background Illumination

### 1.3.3. Surface Bioconjugation

A functionalized surface from 1.3.2, was now bonded to a 150 µm microfluidic channel as in 1.1.2 and incubated for at least 5 h, but mostly over night at 7 °C. Upon finish, microfluidic PTFE-tubing (ID 0.5 mm, Reichelt Chemietechnik) was connected to the inlet and outlet with precision tweezers. Then, the channel was equilibrated with 100 µL to 300 µL MES buffer in a syringe (1 mL, Terumo) with a syringe pump (Fusion 100, Chemyx) with 100 µL min<sup>-1</sup>. Then, 50 mM, 100 mM and 300 mM of EDC and NHS were flushed into the channel with the same flow rate after an dissociation time of 10 min. The channel bottom was incubated for 30 min and then washed again with 100 µL MES buffer.

Subsequently, a desired protein was loaded in high concentration (Neutravidin ( 31050,

Thermo Scientific):  $1 \text{ mg mL}^{-1}$ , Antibody:  $20 \mu\text{g mL}^{-1}$ ), via the tip of a 1 mL syringe or flushed into the channel by vacuum from a microcentrifuge tube. The functionalized channels were now incubated over night in an ice box. Before use, the  $\mu\text{F}$  was washed with  $100 \mu\text{L}$  PBS with 0.02 % nonionic surfactant (Tween 20, Sigma Aldrich) (PBST) for 2 min. Any unreacted binding sites were blocked by a solution of 500 mM ethanolamine hydrochloride (E6133, Sigma-Aldrich) in  $\text{diH}_2\text{O}$  for 30 min. After another washing step, the functionalized channels were further used for either microscope or magnetic bead-capture experiments.

However, in some experiments focus lay on physisorption rather than on chemisorption. Therefore, after the bonding of a microfluidic channel to a non-functionalized substrate, the channel was equilibrated as mentioned before with MES buffer (cave: without surfactant). Then it was incubated with a solution containing protein in highest concentration, p.e.  $1 \text{ mg mL}^{-1}$  neutravidin, at  $7^\circ\text{C}$  over night, while infusing and withdrawing a small volume fraction (approx.  $50 \mu\text{L}$ ) continuously by a syringe pump. Upon finish, the tubing was exchanged with a drop of water at the connection and channel was flushed with PBS carefully at  $50 \mu\text{L min}^{-1}$  to avoid any gas bubbles inside the fluidic. It was stored up to 10 d without any notable decrease in functionality.

#### 1.3.4. Particle Functionalization

Micro- and nanobeads from different suppliers were used in functionalization experiments but modified after the same procedure according to their surface charge. A positive partial charge from an  $-\text{NH}_2$  (amine)-terminated bead and a negative partial charge from a  $-\text{COOH}$  (carboxyl)-terminated bead was used to promote different electrostatic interactions with a microchannel's surface. A list of all used particles and their respective parameters are depicted in table 2.

##### Amine-terminated Beads

For amine beads, NHS-Biotin (203118, Sigma Aldrich) was used for a covalent attachment after the previously mentioned carbodiimide chemistry. Initially, the biotin was dissolved to a concentration of ( $50 \text{ mg mL}^{-1}$ ) in water-free dimethyl sulfoxide (DMSO) and stored upon further use at  $-25^\circ\text{C}$ . The attachment to microbeads was titrated by the molar weight ratio of both reagents and ranged from 10-fold molar excess to a 10 000-fold deficit of biotin over the amine.

In most cases,  $20 \mu\text{L}$  of micromer beads were aliquoted in several microcentrifuge tubes ( $1.5 \text{ mL}$ , Eppendorf) to generate a standard curve of functionalization density later on. NHS-Biotin was diluted to a concentration of  $0.5 \text{ mg mL}^{-1}$  with PBST and vortexed. Then, beads and biotinylation reagent were mixed in the desired ratio thoroughly and incubated for 1.75 h at  $8^\circ\text{C}$  in a shaker (Thermomixer, Eppendorf) at  $1400 \text{ min}^{-1}$ .

Supplier	Brand Name	d ( $\mu\text{m}$ )	Functionalization	Surface Charge ( $\mu\text{mol g}^{-1}$ )	Magnetic Particle Momentum ( $\text{A m}^2$ )
micromod	micromer	8	amine	2.0	0
micromod	micromer-M	8	amine	1.0	$>1.12 \times 10^{-12}$
micromod	micromer	8	carboxyl	2.0	0
micromod	micromer-M	8	carboxyl	1.0	$>1.12 \times 10^{-12}$
invitrogen	Dynabead M280	2.8	streptavidin	0.65-0.90	N.A.
invitrogen	Dynabeads MyOne C1	1.05	streptavidin	$>2.5$	N.A.
Ocean Nanotec	SV0050	0.05	streptavidin	N.A.	N.A.
micromod	BNF-Dextran-redF	0.1	streptavidin	0.2	$>1.27 \times 10^{-16}$
micromod	nanomag-D-spio	0.1	streptavidin	0.02-0.04	$>5.5 \times 10^{-17}$

**Table 2:** Properties of the used microbeads and magnetic nanoparticles (MNPs).

### Carboxyl-terminated Beads

The surface of carboxyl-terminated beads was esterified by EDC-NHS chemistry and covalently bound to amine-PEG<sub>2</sub>-biotin (EZ Link, Thermo Scientific). First, the bead buffer was exchanged to MES buffer with Tween 20 (MEST) with one washing step by centrifugation (as in 1.3.4) to a final bead concentration of  $5 \text{ mg mL}^{-1}$ . 100 mM EDC in diH<sub>2</sub>O and 50 mM NHS in DMSO were prepared and added to the bead solution to a final concentration of 25 mM and 12.5 mM each. The suspension was reacted for 30 min on a shaker at  $1400 \text{ min}^{-1}$  and washed once with MEST buffer. Then, amine-PEG<sub>2</sub>-biotin was added from 10-fold molar excess to a 10 000-fold deficit of biotin over the amine and volume adjusted. The samples were incubated on a shaker for 1.75 h at 8 °C in a shaker at  $1400 \text{ min}^{-1}$ .

### Post-Processing and Characterization of Beads

After the incubation, the beads were washed either magnetically or via pelleting. Magnetic washing was carried out in a magnet stand (), where the beads were separated for 2 min and then washed 3 times with 500  $\mu\text{L}$  to 1000  $\mu\text{L}$  PBST. Pellet washing was

Which company

conducted three times in a table centrifuge (Fresco 17, Thermo Scientific) at 800 x g to 1200 x g for 10 min. The supernatant was discarded and the pellet was dissolved in 500  $\mu\text{L}$  to 1000  $\mu\text{L}$  PBST. After both washing procedures, the beads were resuspended in 100  $\mu\text{L}$  MACS or PBST and stored at 4  $^{\circ}\text{C}$ .

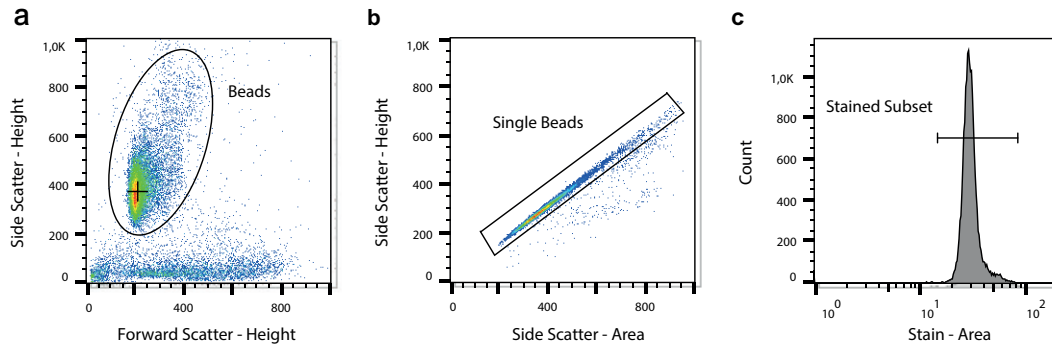


**Figure 2: Gating Strategy for Biotinylated Beads**

**a**, In the forward-side-scatter plot, the general bead population with high side scatter is selected from the background. **b**, Single beads are differentiated by their sphericity, their ratio of height:area in the side scatter. Points on the line through the origin are spherical. **c**, The stained subset in the respective color is now selected and the median fluorescence intensity (MFI) as well as the coefficient of variance (CV) is computed.

Characterization of any surface modification was done via fluorescence-flow cytometry or -microscopy. 30 000 beads to 60 000 beads were diluted to 20  $\mu\text{L}$  and incubated with 100 ng streptavidin-atto488 (49937, Sigma Aldrich) or Anti-Biotin-PE (Miltenyi) for 30 min at 8  $^{\circ}\text{C}$  in a shaker. The beads were then diluted to a final volume of 100  $\mu\text{L}$ , transferred to a 96-well plate (TPP) and measured in the autosampler of a flow cytometer (MACS Quant Analyzer 10, Miltenyi). Following parameters were held constant over all measurements: *Flow Rate*: High, *Mix Sample*: Strong, *Mode*: Standard, *Uptake/Sample Volume*: 100  $\mu\text{L}$ . The photomultiplier voltages of forward and side scatter were lowered in most experiments by 10 V and 120 V respectively due to the homogeneous and reflective nature of the particles. Data analysis was performed by FlowJo (10.6.2, Becton Dickinson) after a gating strategy which is depicted in Fig. 2. For fluorescence microscopy, the beads were stained with streptavidin-atto488 after the same procedure and imaged statically on a covered microscope slide at an exposure time of  $>100\,000\,\mu\text{s}$  and a gain  $>15$ . Images were then processed by Fiji. In both measurements, the resulting data was plotted in Origin (2020b, OriginLab).

### Coating of Biofunctionalized Non-Magnetic Beads with Magnetic Nanoparticles

The biotinylated, non-magnetic microbeads (Table 2) were coated covalently with different MNPs in order to establish a bead-side titration of binding sites. Therefore, 5  $\text{mg mL}^{-1}$  biotinylated beads in PBST were equilibrated for 10 min and mixed with 7.5  $\mu\text{g}$  BNF-dextran-redF-streptavidin / nanomag-D-spio, 6  $\mu\text{g}$  of SV0050 or 10  $\mu\text{g}$  Dynabeads C1 over night on a shaker. Afterwards, the supernatants were exchanged twice by careful centrifugation to avoid sedimentation of the nanoparticles.